Configuration and Analysis of a High Impedance Fault Simulation Model

Gabriela N. Lopes * **Luiz H. P. C. Trondoli** * **Jose C. M. Vieira** *

* *Departament of Electrical and Computer Engineering, São Carlos School of Engineering, Univeristy of São Paulo, São Carlos, SP (e-mail: gabrielanuneslopes@usp.br, luiz.trondoli@gmail.com, jcarlos@sc.usp.br)*

Abstract: When the contact between an energized conductor and a high impedance surface occurs, a High Impedance Fault (HIF) is generated. It can cause interruption of electrical power supply, bushfires, and dangers to living beings. Even being a well-known and studied problem, there is still a need to develop more effective HIF protection schemes. To test these new techniques, HIFs' current signals are necessary. However, obtaining real measurements during the fault occurrence can be challenging. To solve this issue, tests are usually performed using computational models to represent the real HIF features as detailed as possible. However, setting the HIF models parameters can be a hard task. To solve this issue, this paper presents a methodology to extract the parameters of real HIF signals to use a complete and recently-developed HIF model and validate its use in a Distribution System (DS). Tests are carried out analyzing the harmonic and interharmonic content of the signals measured in the DS. The main goal is to help researchers use the HIF model in new scenarios, improving the quality of the tests of new and existing HIF protection schemes.

Keywords: high impedance fault; fault model; distribution systems.

1. INTRODUCTION

High Impedance Faults (HIFs) occur in Distribution Systems (DSs) due to the contact between electrical network conductors and high impedance surfaces. HIFs can cause interruptions in the electricity supply and cause several hazards, such as the risk of electric shock to humans and animals, as well as generating bushfires (Costa et al., 2015; Gomes et al., 2017). The HIFs low fault current (due to the high contact impedance) hinders conventional protection from correctly functioning (Depew et al., 2006; Lima et al., 2016). Nowadays, there is no fully effective HIF protection methodology, so researchers are still developing solutions.

When researchers develop new HIF protection techniques, they have to evaluate the methodology by performing tests that must consider the HIFs occurrence as they take place in real systems. However, obtaining real HIF signals to test new algorithms can be dangerous and difficult. Consequently, most of the HIF protection algorithms are tested using models that emulate the behavior of this type of fault in simulation software. Thus, to develop models that replicate the HIFs, the characteristics of the electrical signals during HIFs must be modeled, such as low current amplitude, non-linearity between current and voltage, buildup, asymmetry, shoulder, intermittence and randomness (Costa et al., 2015).

Several HIF models have been developed in the literature. There are simple models, based on an impedance of high value, and also modern methodologies, which represent the HIF characteristics set by the user, including the arc randomness. An example is the HIF model proposed by Trondoli et al. (2022), which makes it possible to reproduce the HIF characteristics individually or simultaneously. Furthermore, they can occur randomly over time, a characteristic similar to real HIF signals. However, in Trondoli et al. (2022), the configuration of the model was carried out by using only one real HIF current. So, the procedures to configure the HIF model proposed in Trondoli et al. (2022) considering various types of soils and its use in a DS have not been fully described so far.

This paper proposes the analysis and configuration of the HIF model proposed by Trondoli et al. (2022) using real HIF signals. Additionally, simulations are performed using the IEEE 34-node test system, varying the fault incidence bus, to demonstrate the model's application. As the model generates random features, a statistical analysis of the harmonics and interharmonics extracted from the signals during the HIF occurrence is performed. The main goal is to help researchers use the model in HIF simulations, characterizing the fault through the measured signals and validating the model in tests systems.

This paper is divided as follows: Section 2 presents a literature review on the HIFs characteristics and the main HIF models. Section 3 shows the study methodology, including the parameters extraction process. Section 4 presents the analysis of the current's harmonics and interharmonics when varying the model parameters and the HIF location so that, lastly, Section 5 can conclude the study.

2. HIGH IMPEDANCE FAULTS MODELS

In order to represent any natural phenomenon, it is necessary to develop models that express its behavior as similarly as possible. Hence, modeling HIFs became an important issue in power systems protection studies due to the difficulty of performing real tests in different conditions. Employing models that satisfactorily represent the fault is fundamental to testing new HIF protection algo-

⋆ Financed by the Coordination for the Improvement of Higher Education Personnel-Brazil (CAPES)-Finance Code 001, by Brazilian National Council for Scientific and Technological Development (CNPq) Grant 304900/2018-4 and by grant 2020/06935-5, São Paulo Research Foundation (FAPESP).

rithms using DSs simulation software. For such modeling to occur satisfactorily, it is necessary to study the main characteristics related to the fault.

The HIFs study starts with their occurrence. The HIFs occur by contact between an energized conductor and a high impedance surface. Such a surface is usually vegetation, sand, clay, cement, asphalt, grass, etc. (Macedo et al., 2015; Costa et al., 2015). These surfaces cause different characteristics to the signals. Thus, to enable the studying HIFs, researchers established the main features present in the signals measured during HIFs, so that protection algorithms and models can emulate their behavior. Figure 1 shows the main HIF characteristics, which are defined as follows (Nakagomi, 2006; Costa et al., 2015):

- **Low fault current**: due to contact with a high impedance surface. It prevents HIF detection by conventional overcurrent protection;
- **Long duration:** while the material is burning, the electric arc remains;
- **Waveform distortion:** occurs due to the non-linearity of the electrical arc resistance and implies in low order harmonics;
- **Asymmetry between half-cycles**: the current has different amplitudes at each half-cycle. It implies even harmonics;
- **The *build-up***: progressive increase in current amplitude from the beginning of the fault;
- **The *shoulders***: periods the fault current stabilizes;
- **Modulation:** the modulation occurs by the progressive variation of the fault current amplitude over time;
- **Avalanche:** when the voltage crosses zero, since the conductor is in contact with the surface, the high resistance prevents current from flowing. When the voltage is sufficient to increase the electric field around the conductor, the electrons accelerate, ionize the air, and produce the fault current.
- **Intermittence:** periods when the fault current is extinguished, with subsequent re-ignition. It implies high-frequency components;
- **Randomness:** all of the above characteristics occur randomly due to the electric arc dynamic.

Once the main HIF characteristics are defined, the models that emulate them can be analyzed. Thus, one of the simplest approaches to model the HIFs was used by Nakagomi (2006). The fault is modeled by a resistance, as normally done for low impedance faults, using a high ohmic value. However, it does not reproduce any HIF characteristics besides the low fault current, making this representation unfeasible for practical applications. The first model to emulate the HIF features was proposed by Emanuel et al. (1990). It uses an impedance in series with two DC sources in anti-parallel. Thus, it is possible to reproduce the effect of asymmetry and avalanche.

Inspired by Emanuel et al. (1990), several other models have emerged, such as the one presented in Lai et al. (2005). The modification is using two linear resistors instead of a series impedance. Thus, in addition to the avalanche, it reproduces asymmetry variation. Another example is the Wai and Yibin (1998) model, which replaces the DC sources with sawtooth sources. The goal was to better represent the dynamics of the electric arc. Despite this, the features are repeated over time, maintaining the signals deterministic. Both models do not reproduce other HIF effects, such as buildup and shoulder. However, there are models that reproduce both features. An example is Nam et al. (2001), which uses two variable resistors in series to replace the series impedance. Nonlinear resistors are configured with real HIF signals. Despite its contributions, nonlinearity and asymmetry are the same in all cycles, not representing the randomness they occur, generating the same fault signal at each simulation.

Other authors have proposed improvements to the HIF representation, including randomness to the model. In the model used in Sheng and Rovnyak (2004), the change is based on the use of non-linear resistors and variable amplitude of the DC sources. In Sedighi and Haghifam (2010), it is proposed to use models of Lai et al. (2005) connected in parallel, which are randomly connected to the network through switches. Thus, both models introduce randomness to the signal. However, they do not reproduce buildup, shoulders and intermittence.

Also, some models are not based on Emanuel et al. (1990) but on models of electric arc conductivity proposed in Mayr (1943), named Cassie and Mayr Model. One of them is used in Torres-Garcia et al. (2020). They modify the electric arc conductivity equation by using only one resistor, which reproduces most of the HIF characteristics by following the electric arc equation's behavior. However, to parameterize it, real signals are needed, and the same HIF signal is generated for each of them.

In contrast, the Trondoli et al. (2022) model was recently proposed. This model was based on the Emanuel model. However, the user can control the HIF features, and random signals are generated in each simulation. Thus, it reproduces the buildup, shoulder, asymmetry, avalanche, intermittence, and modulation, all of which can be generated simultaneously or separately and occur randomly through probabilities defined by the user. Figure 2 illustrates the electrical components of some of the main HIF models in the literature. It is possible to notice the evolution in the HIF modeling and highlight that, by adding the reproduction of each characteristic, it is possible to develop models increasingly similar to real HIFs.

3. METHODOLOGY

This section describes the methodology to configure the model of Trondoli et al. (2022), its application in a DS, and the signal's analysis. The software used in the simulations is the Alternative Transients Program (ATP) through the ATPDraw interface (ATPDraw, 2017). The signal processing analysis are carried out using Matlab.

3.1 Parameters Extraction

The model developed by Trondoli et al. (2022) and validated in this paper has as main feature to represent the HIF characteristics maintaining the randomness present in this type of fault. It uses controlled resistances and switches to emulate the HIF behavior. In general, the user must establish the parameters presented in Table 1. Each of these parameters must be set by the user and may be present simultaneously or individually. It is possible to configure it using real signals. Thus, the methodology for extracting parameters from real signals can be followed according to the following steps (Trondoli et al., 2022):

(1) Choose a representative time window of the real signal containing the HIF characteristics - including the buildup and some cycles of modulation;
(2) Calculate the signal envelope as each half-cycle peak current;
(3) Calculate $iFault$ as the median of the envelope value;

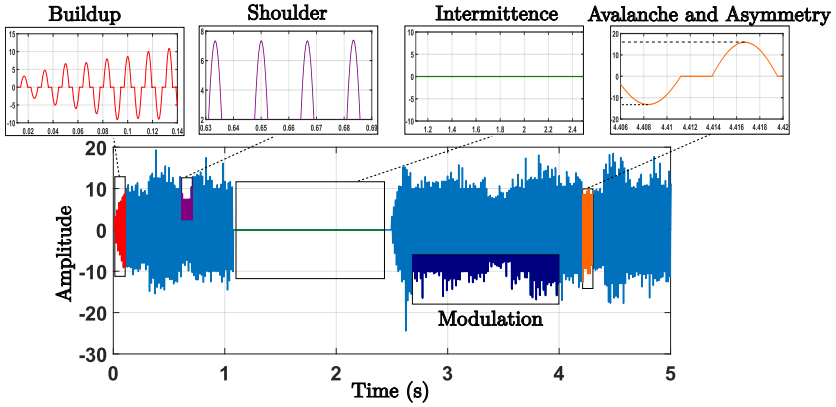

Figure 1. High Impedance Faults Characteristics.

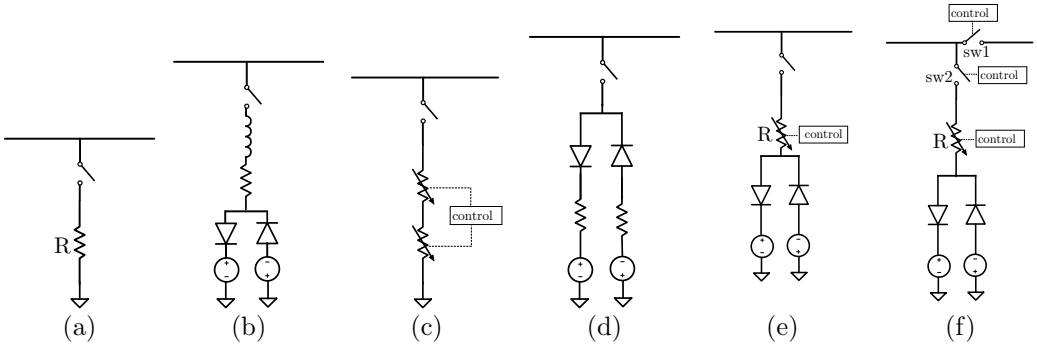

Figure 2. Some of the main HIF models, based on (a) Nakagomi (2006),(b) Emanuel et al. (1990), (c) Nam et al. (2001), (d) Lai et al. (2005), (e) Sheng and Rovnyak (2004) e (f) Trondoli et al. (2022).

Table 1. HIF Parameters set in the HIF model of Trondoli et al. (2022).

Parameter	Description	Unity
vl	System line voltage	[V]
$pAsy$	Probability that asymmetry occurs	[%]
$freq$	System frequency	[Hz]
$iSpike$	Maximum spikes current (API*)	[%]
vp	Positive DC voltage source	[V]
$pSpike$	Probability that spikes occurs	[%]
$soil$	Soil type	-
$iPosMod$	Maximum current modulation (API)	[%]
$rupt$	Instant of cable rupture	[s]
$pPosMod$	Probability that Imod* is greater than $iFault$	[%]
$touch$	Instant the cable touches the ground	[s]
$iNegMod$	Minimum current modulation (API)	[%]
$iFault$	Steady-state peak fault current	[A]
$pNegMod$	Probability of Imod being lower than $iFault$	[%]
$cBup$	Number of buildup cycles	-
$mincy$	Minimum number of shoulder cycles	-
$iPerc$	Initial arc current (API)	[%]
$maxcy$	Maximum number of shoulder cycles	-
$iAsy$	Maximum asymmetry current (API)	[%]

*API - as percentage of $iFault$/ Imod - current modulation

(4) Obtain $cBup$ by calculating the number of cycles until the peak current is greater than $iFault$ for two consecutive cycles;
(5) Calculate $iPerc$ as the ratio between the peak currents of the first and last buildup cycle;
(6) Calculate the asymmetry by the peak current difference between half-cycles.
(7) Obtain the signal without asymmetry calculating the signal minus the asymmetry values.
(8) Separate the asymmetry values between those greater (spikes) and lower (asymmetry) than twice the average asymmetry;
(9) Calculate $iAsy$ e $iSpike$ as the maximum values of asymmetry and spikes, respectively. They are both given as a percentage of $iFault$.
(10) Considering all cycles of the chosen HIF signal, calculate $pAsy$ as the probability that $iAsy$ occurs and $pSpike$ as the probability that $iSpike$ occurs;
(11) Calculate the signal modulation as the average peak current for four consecutive cycles of the signal without asymmetry;
(12) Divide the modulation values between those greater (positive) and lower (negative) than $iFault$;
(13) Calculate $iPosMod$ and $iNegMod$ as the difference between the positive and negative values and $iFault$, respectively;
(14) Obtain $pPosMod$ and $pNegMod$ as the probability of the modulation values being greater or lower than $iFault$, respectively.
(15) Calculate $mincy$ and $maxcy$ as the minimum and maximum number of cycles that the modulation values have equal values considering a tolerance of 1%.

After calculating the parameters, it is possible to use the model in several systems and conditions.

3.2 Application of the HIF Model in a Test System

In Trondoli et al. (2022), only a fictitious one-node system is used to connect the model. In this paper, the IEEE 34-nodes test system (Figure 3) is used to expand the model application and analyze its interaction with a DS. The IEEE 34-nodes test system has distributed loads, transformers, regulators, and natural unbalance (IEEE Distribution System Analysis Subcommittee, 2010). In this paper's study, all measurements were performed at bus 800 (the substation bus).

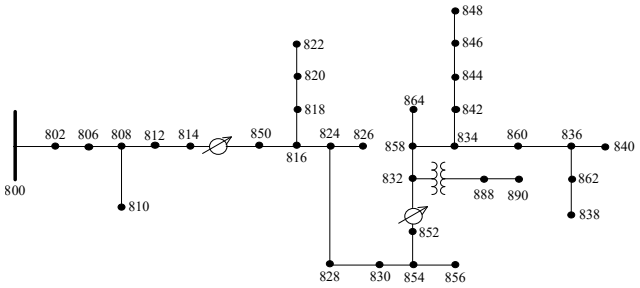

Figure 3. IEEE 34-node test system.

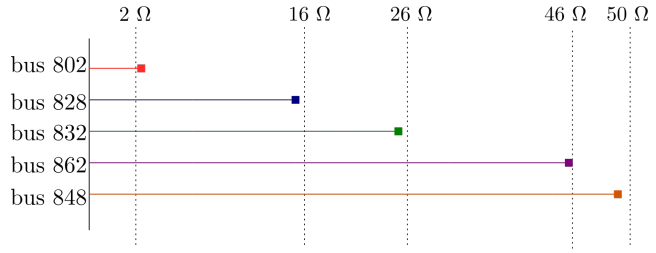

Figure 4. Electric distance between the measurement location and the HIF incidence buses.

The Algorithm 1 shows the pseudocode of the simulation scenarios. Thus, the incidence of HIFs was studied in five system buses: 802, 828, 832, 838, and 842. These buses were chosen because they show the HIF influence on the measured signals along with the system, as they present different electrical distances until the measurement location (substation), as shown in Figure 4. Additionally, the simulations were repeated for Y times, as the model generates different signals with the same set of parameters. The signal analysis is performed by extracting the current signals' frequency content using the Fourier Transform.

Algorithm 1 Algorithm for the generation of the HIF data set in different scenarios.

```
HIF incidence buses ← 802, 828, 832, 838, 842
Real signals used to configure ← 1 to X
Simulations using the same parameters ← 1 to Y
for All Incidence Buses do
  for All Parametrization Values do
    for All HIF simulations using the same parameter do
      Create a new ATP card adding the modifications
      Run the new ATP card and save the signals
    end for
  end for
end for
```

4. RESULTS AND ANALYSIS

This section shows the results of the HIF model configuration. Firstly, the parameters are extracted from the real signals. The real HIF current signals were provided by the authors of Macedo et al. (2015). They were recorded at the fault spot in a medium voltage DS (13.8 kV). The tests consisted of breaking an energized conductor, which falls into the ground containing different surfaces, such as sand, grass, clay, cement, gravel, and asphalt. Therefore, ten real signals acquired at 128 samples per cycle were selected for the study of this paper, whose current waveforms recorded at the fault spot are shown in Figure 5. Note that the signals have several HIF characteristics, which occur randomly during the fault.

The chosen real HIF signals were used as base signals to extract the parameters used in the HIF model. The HIF model generates random signals through the set probabilities. Consequently, different HIF signals are generated each time it is used, keeping the HIF characteristics. Therefore, the simulation was repeated ten times for each base signal. Summarizing, simulations were performed considering the HIF incidence on five system buses (the model was connected to phase A), using ten sets of parameters and repeating each scenario ten times, totaling 500 simulations. Thus, 500 faulted phase current signals were analyzed.

4.1 Parameters extracted from the real signals

Table 2 shows the parameters extracted from the real HIF signals (the base signals) using the proposed methodology. The variable parameters were established according to the extraction steps explained in Section III. Note that the parameters differ markedly among the signals, which shows that the HIF signals are random and variable. The parameters that remain constant are the system voltage (24.9 kV), the system frequency (60 Hz), the pickup voltage (5 kV) (value set according to Emanuel et al. (1990)), and the *rand* variable, which was set to 1. Thus, the features occur randomly across the signal, just as they do in real signals. The rupture and touch times (1 and 2.28 s, respectively) were established considering that the conductor breaks in 1 second of simulation, and after 1.28 s of fall, it contacts the surface. The fall time was established considering that a 8m height of the primary network to the ground using the free-fall equation.

4.2 Test system results

This section presents the results of the tests and the analysis of the current signals measured during the HIFs in all set scenarios. Thus, as an example, Figure 6 shows the different current signals measured at the system substation when using the base signal 1 (see Table 2) to set the parameters of the model in each of the analyzed locations. In the simulations, the system's steady-state is up to 1 s. From 1 s to 2.28 s, the conductor falls, and from that period onwards, the HIF starts. Note that when the fault occurred at bus 802 (the closest to the substation), the HIFs characteristics were remarkable. However, when the fault occurs at a greater distance from the substation, it becomes more difficult to identify, as shown by Lopes et al. (2022) when using a current source to inject real HIF signals directly into the system. Thus, the analysis of Figure 6 reveals that the model is able to reproduce the HIF features when interacting with the DS.

The proposed methodology is based on analyzing the signals' frequency content to evaluate the model and its interaction with the system. It is based on the HIFs intrinsic characteristics to cause non-linearity in electrical signals during their occurrence. Furthermore, several papers in the literature base their methods on the signal's frequencies, which change in DSs when HIFs occur.

Signals processing techniques are the main tools to extract a signal's frequency content. In this paper, the analysis uses the Discrete Fourier Transform (DFT), which is widely used in protection relays and HIF protection methods. Thus, as in Trondoli et al. (2022), the HIF analysis is based on the low order harmonics amplitude, which occurs due to signal distortion and asymmetry, and the interharmonics, which emerge due to the buildup (Lopes et al., 2022; Macedo et al., 2015; Soheili et al., 2018).

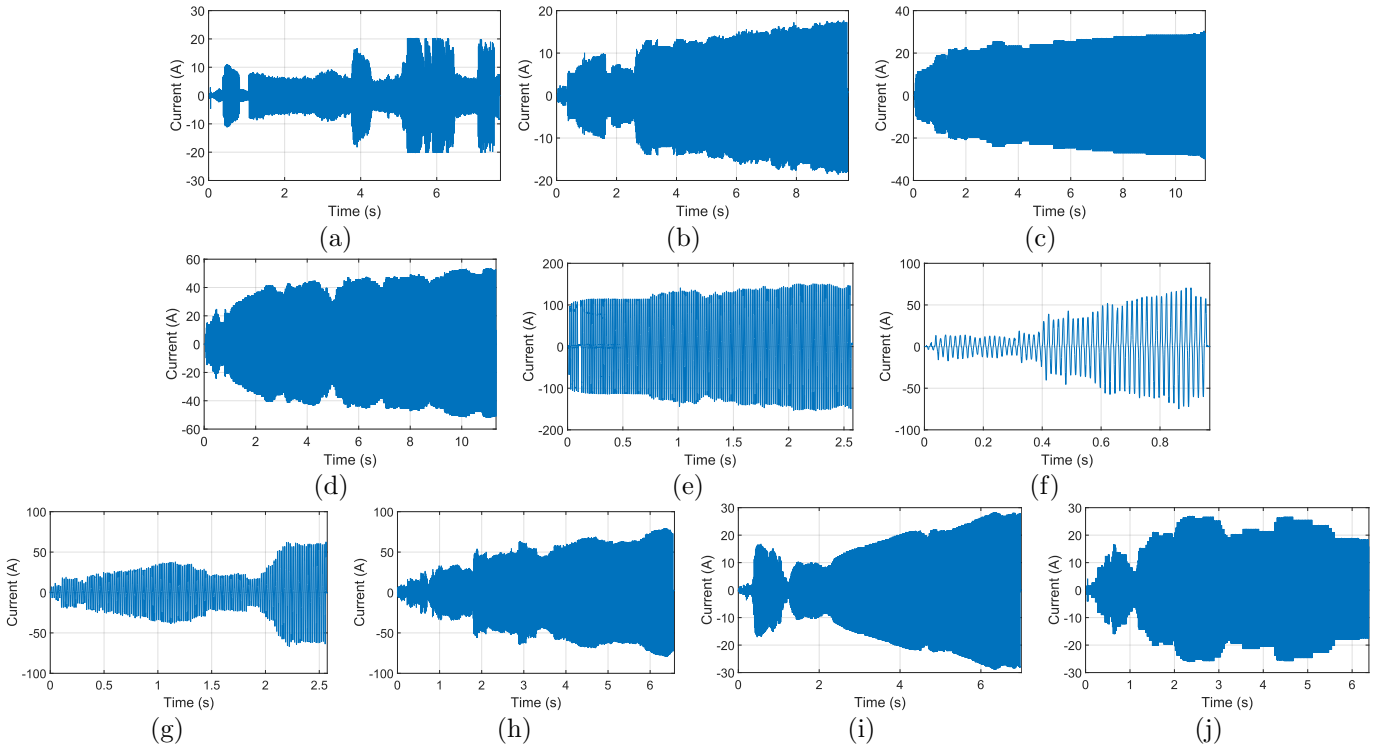

Figure 5. Formas de onda das correntes reais de FAI utilizadas para parametrizar o modelo nos testes. POR EM INGLES

Table 2. Parameters set in the model extracted from each real HIF signal.

	Real Signals									
Parameters	**1**	**2**	**3**	**4**	**5**	**6**	**7**	**8**	**9**	**10**
vl **(V)**	24900	24900	24900	24900	24900	24900	24900	24900	24900	24900
$freq$ **(Hz)**	60	60	60	60	60	60	60	60	60	60
vp **(V)**	5000	5000	5000	5000	5000	5000	5000	5000	5000	5000
$ruptt$ **(s)**	4	1	1	1	1	1	1	1	1	1
$toucht$ **(s)**	2.28	2.28	2.28	2.28	2.28	2.28	2.28	2.28	2.28	2.28
$ifault$ **(A)**	9.54	12.34	23.91	40.32	128.61	35.16	31.26	49.18	17.22	19.61
$iperc$ **(%)**	0	0	0	0	53	8	20	11	0	0
$cbup$	26	179	181	144	52	34	57	113	208	91
$soil$	2	2	2	2	2	2	2	2	2	2
$Iasy$ **(%)**	14.25	12.33	6.78	8	3.33	21.12	8.56	4.39	5.56	7.01
$Ipeak$ **(%)**	59.88	106.86	9.05	13.42	9.80	28.52	19.83	26.17	60.83	0
$pIasy$ **(%)**	84.90	66.42	72.44	76.48	59.41	36.11	53.74	62.84	48.98	75.78
$pIpeak$ **(%)**	9.12	2.74	0.30	2.06	5.81	3.44	8.42	8.11	1.19	0
$Modneg$ **(%)**	50	50	50	28.74	15.57	16.49	50	23.95	50	10.47
$Modpos$ **(%)**	50	39.19	19.60	27.78	15.96	50	50	50	50	31.94
$pModneg$ **(%)**	30.40	58.20	53.88	55.89	45.20	17.20	32.37	50.68	49.68	52.27
$pModpos$ **(%)**	65.14	11.98	19.46	22.06	19.37	17.20	32.37	20.27	2.38	23.52
$mincy$	10	10	10	10	10	0	10	10	0	10
$maxcy$	10	10	80	10	10	0	10	10	10	20
$rand$	1	1	1	1	1	1	1	1	1	1

4.3 Analysis of the harmonics

Thus, to analyze the harmonics of the signals during the HIF (after 2.28 s), the next steps were followed:

- Using the DFT, calculate the harmonics of each signal with a one-cycle window shifting each cycle;
- Calculate the average harmonic amplitude considering the entire fault duration and normalize it in relation to the fundamental component;
- Analysis I: Evaluate the average harmonic amplitude statistically considering the HIF in different locations;
- Analysis II: Calculate the average harmonic amplitude among all the generated signals (regardless of the parameters) in each HIF location.

Starting with analysis I, Figure 7 shows the boxplot of extracted harmonics of all the signals generated by base signals 1, 2, and 3 (see Table 2) considering the HIF incidence at bus 802 (the closest to the measurement) and bus 848 (the farthest). The blue box shows the limit between the amplitude of the respective harmonic, considering the signals generated by the model with the same parameters. The red line is the median amplitude, and the black lines show the maximum and minimum values. The results show that when the fault occurred at bus 802, even with the probabilities considered, the amplitude of the harmonics presented very close values, demonstrating low dispersion. When the most distant bus was considered, the dispersion of values increased. Thus, with the same parameters, the model reproduced the nonlinear characteristics that imply the low order harmonics of the measured current signals, and they could be identified even with the system loads interference.

Figure 8 shows the results of analysis II, considering the average harmonic energy of all 100 signals evaluated (10 base signals generating 10 HIF signals) in each of the five incidence buses. The results reveal a great variance in the amplitude of the 2^{nd}, 3^{rd}, 5^{th}, and 7^{th} harmonic orders.

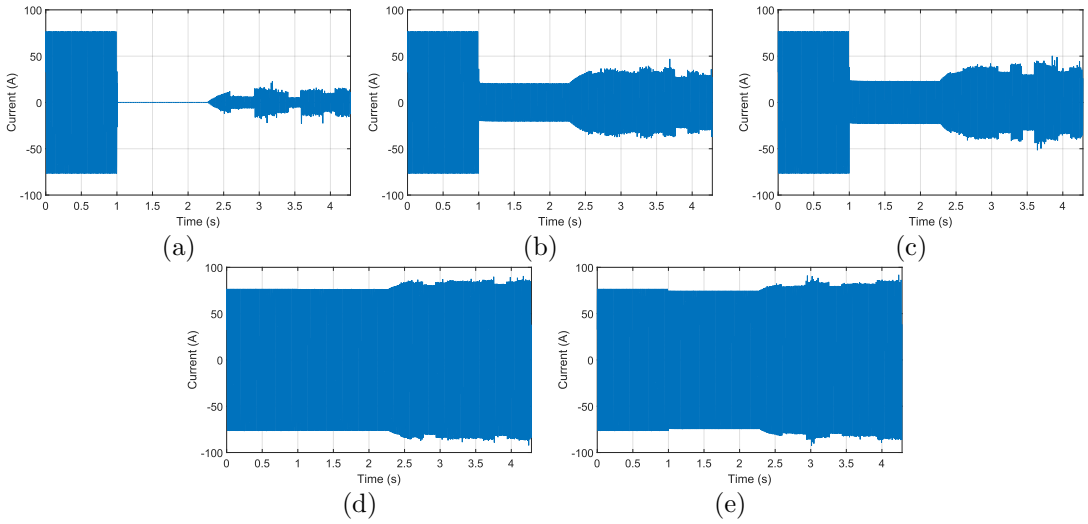

Figure 6. Waveforms of the current measured at the system substation when the parameters extracted from the base signal 1 were set on the HIF model connected to the buses (a) 802, (b) 828, (c) 832, (d) 862 and (e) 848.

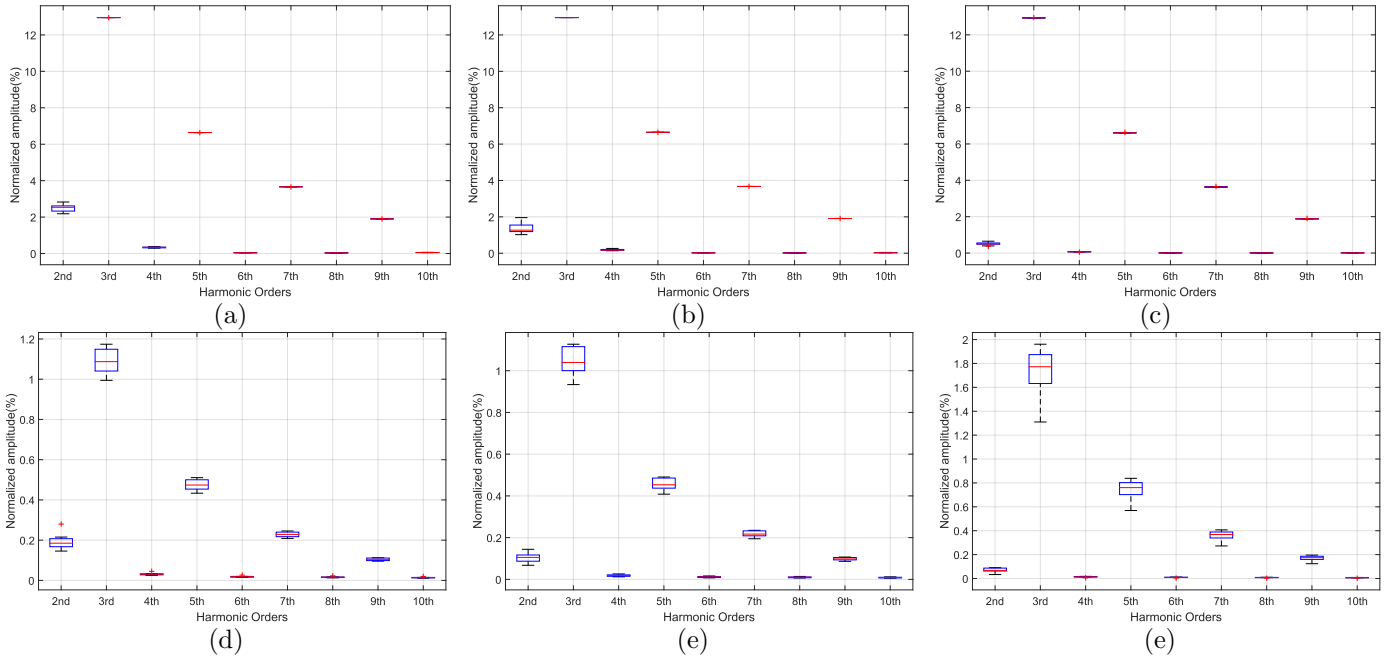

Figure 7. Average harmonic amplitude of the current signals measured during the HIF incidence at bus 802 considering the parameters extracted from the base signals (a) 1, (b) 2, and (c) 3, and with the HIF incidence at bus 848 considering the parameters of the base signals (d) 1, (e) 2 and (f) 3.

This result is justified since this figure shows results based on HIFs in different soils, with varying probabilities. It is also noted that there was a greater amplitude of harmonics (in relation to the fundamental) in the buses closest to the substation compared to the farthest ones, which would facilitate fault identification by methods based on harmonics at these locations. In general, it was possible to extract the frequencies in all conditions, showing that the model satisfactorily characterized the HIF event.

4.4 Analysis based on Interharmonics

According to Macedo et al. (2015), the interharmonics are present mainly around the signal's fundamental component (in this case, 60 Hz) due to the HIF current amplitude variation during the buildup. There is a constant increase in the current during this period until the fault current is reached. Hence, the analysis of the signals interharmonic content obeyed the following steps:

- Calculate the interharmonics of the first second of fault using a 60-cycle window, obtaining a frequency resolution of 1 Hz;
- Normalize the interharmonics amplitude by the amplitude of the fundamental component of the signal;
- Calculate the energy ϵ of the interharmonics h trough Parseval's Theorem (Lathi and Green, 2005):

$$\epsilon_{period} = \sum_{k=k_i}^{k_f} |Amp(h)|^2 \quad (1)$$

the periods A and B include the interharmonics k_i and k_f from 40 to 56, and 64 to 80 Hz, respectively.

- Calculate the interharmonic energy, as:

$$IH_e = \epsilon_A + \epsilon_B \quad (2)$$

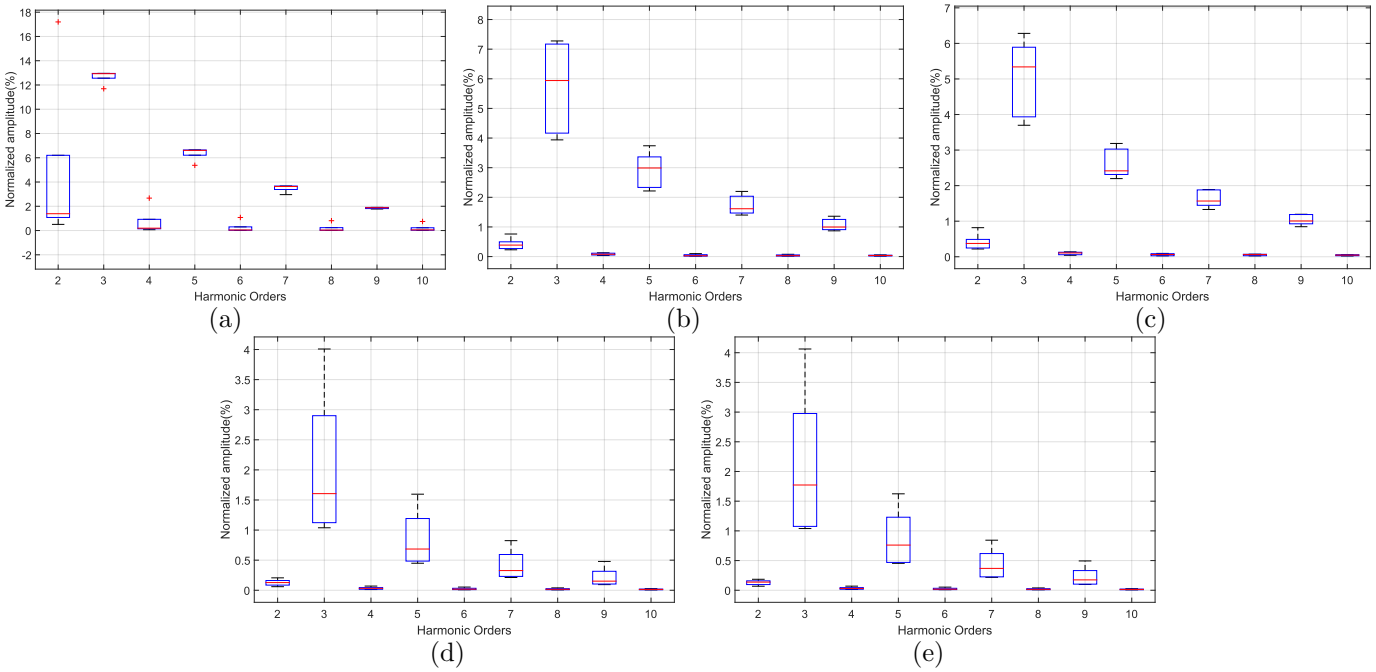

Figure 8. Average harmonic amplitude of the current signals recorded when the HIF occurred using the model by Trondoli et al. (2022) at the buses (a) 802, (b) 828, (c) 832, (d) 862 and (e) 848.

- Calculate the average interharmonic energy IH_e index for all the signals generated using the same parameters (same base signal);

Figure 9 shows the average interharmonic energy IH_e considering the HIF model configured with the ten base signals connected to the five analyzed system buses. The results proved the existence of interharmonic energy in all analyzed signals, showing the buildup influence on the current measured at the substation. Also, the interharmonic energy presents a greater value when the HIF occurs in the buses close to the substation. For example, considering the HIF signals generated with the parameters extracted from the base signal 1, the median interharmonic energy is approximately 2.2% of the fundamental when the HIFs occur at bus 802. However, it decreases to approximately 0.2% when the HIFs occur at buses 828 and 832 and to approximately 0.015% at buses 862 and 848. Such a feature was expected and similar to real signals, as the lower the number of loads between the faulty spot and the measurement, the higher the HIF characteristics influence the current signals measured at the system substation.

5. CONCLUSION

This paper presented the parameter extraction process and statistical analysis of harmonics and interharmonics of current signals recorded during the HIFs occurrence using the Trondoli et al. (2022) model. First, a review of the HIF characteristics showed the need to replicate them in HIF simulation models. Then, a methodology to extract the model parameters from real signals was presented. The tests were performed connecting the HIF model to system buses and recording the current during its occurrence.

The results showed that low-order harmonics are present in all generated signals. Even with different probabilities, there was low variance in the amplitude of the harmonics in buses close to the measurement. However, the amplitude dispersion increased in distant buses, showing that the interaction with the system loads modifies the currents signals measured at the system substation during HIFs. The results also showed that interharmonics were also present in all analyzed signals due to the model's ability to replicate the HIF signal buildup. The interharmonics energy decreased when considering greater distances from the substation. The study proved that the model is able to replicate the HIF characteristics while maintaining its inherent randomness even when applied to a test system.

This study provided a methodology to use a complete model for simulating HIFs. It fully represents the real HIF characteristics, allowing the analysis of the DSs during the HIF simulation. Thus, increasingly robust protection methods can be developed, even for authors who do not have access to real HIF signals under different conditions.

ACKNOWLEDGMENT

We would like to thank the authors of Macedo et al. (2015) for providing the real HIF data.

REFERENCES

ATPDraw (2017). *ATPDraw - The graphical preprocessor to ATP Electromagnetic Transients Program.*

Costa, F.B., Souza, B.A., Brito, N.S., Silva, J.A., and Santos, W.C. (2015). Real-time detection of transients induced by high-impedance faults based on the boundary wavelet transform. *IEEE Trans. on Industry Applications*, 51(6), 5312–5323. doi:10.1109/TIA.2015.2434993.

Depew, A.C., Parsick, J.M., Dempsey, R.W., Benner, C.L., Don Russell, B., and Adamiak, M.G. (2006). Field experience with high-impedance fault detection relays. In *Proceedings of the IEEE Power Engineering Society Transmission and Distribution Conference*, 868–873. IEEE, College Station, TX, USA. doi:10.1109/TDC.2006.1668612.

Emanuel, A.E., Cyganski, D., Orr, J.A., Shiller, S., and Gulachenski, E.M. (1990). High impedance fault arcing on sandy soil in 15 kV distribution feeders: contributions to the evaluation of the low frequency spectrum. *IEEE Transactions on Power Delivery*, 5(2), 676–686.

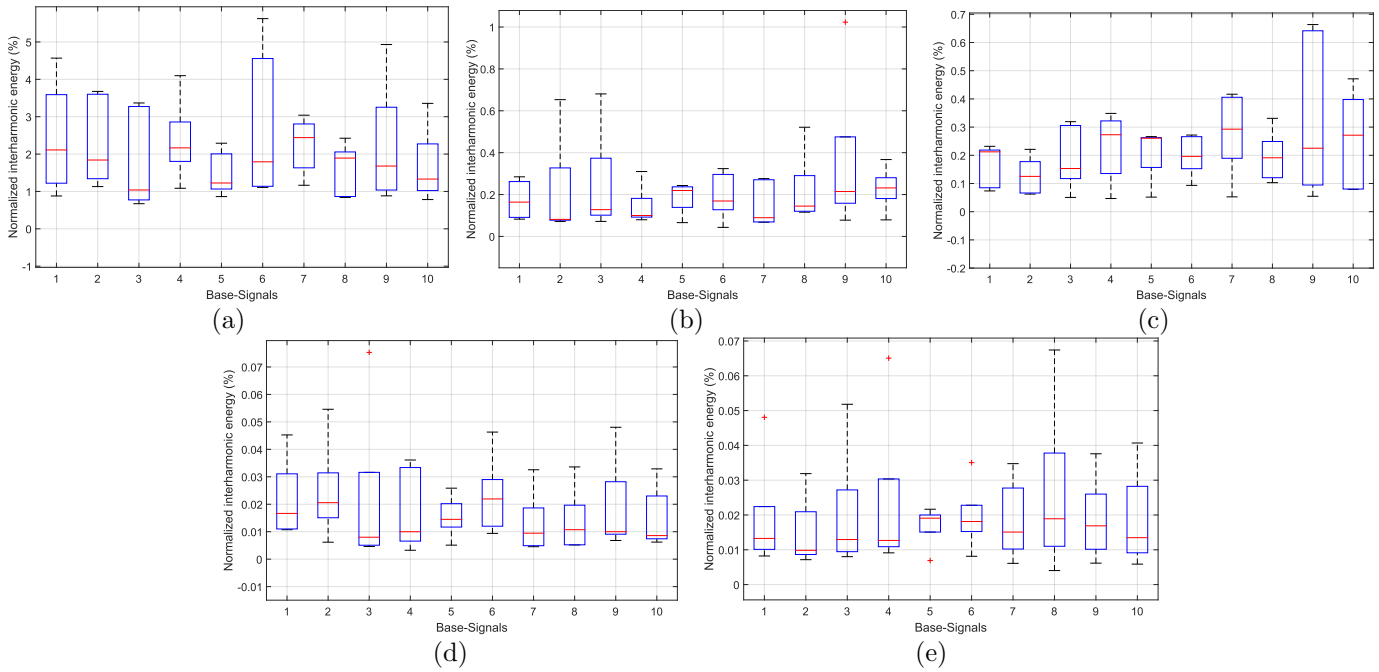

Figure 9. Interharmonic energy considering the ten base signals when the HIF occurs at buses (a) 802, (b) 828, (c) 832, (d) 862 and (e) 848.

Gomes, D.P.S., Ozansoy, C., and Ulhaq, A. (2017). High-Frequency Spectral Analysis of High Impedance Vegetation Faults on a Three-wire System. In *2017 Australasian Universities Power Engineering Conference (AUPEC)*. IEEE, Melbourne, VIC, Australia. doi:10.1109/AUPEC.2017.8282456.

IEEE Distribution System Analysis Subcommittee (2010). *IEEE 34 Node Test Feeder*. EUA. URL `http://sites.ieee.org/pes-testfeeders/resources/`.

Lai, T.M., Snider, L.A., Lo, E., and Sutanto, D. (2005). High-impedance fault detection using discrete wavelet transform and frequency range and rms conversion. *IEEE Transactions on Power Delivery*, 20(1), 397–407.

Lathi, B.P. and Green, R.A. (2005). *Linear systems and signals*, volume 2. Oxford University Press New York, EUA.

Lima, É.M., Brito, N.S.D., Souza, B.A.d., Santos, W.C.d., and Fortunato, L.M.d.A. (2016). Analysis of the influence of the window used in the Short-Time Fourier Transform for High Impedance Fault detection. 350–355. IEEE, Belo Horizonte, Brazil. doi:10.1109/ICHQP.2016.7783465.

Lopes, G., Menezes, T., Santos, G., Trondoli, L., and Vieira, J. (2022). High impedance fault detection based on harmonic energy variation via s-transform. *International Journal of Electrical Power Energy Systems*, 136, 107681. doi:https://doi.org/10.1016/j.ijepes.2021.107681.

Macedo, J.R., Resende, J.W., Bissochi, C.A., Carvalho, D., and Castro, F.C. (2015). Proposition of an interharmonic-based methodology for high-impedance fault detection in distribution systems. *IET Gener. Transm. Distrib.*, 9(16), 2593–2601. doi:10.1049/iet-gtd.2015.0407.

Mayr, O. (1943). Beiträge zur theorie des statischen und des dynamischen lichtbogens. doi:10.1007/BF02084317.

Nakagomi, R.M. (2006). *Proposição de um Sistema para Simulação de Faltas de Alta Impedância em Redes de Distribuição*. Ph.D. thesis, Universidade de São Paulo. doi:10.11606/D.3.2006.tde-15122006-103128.

Nam, S.R., Parkn, J.K., Kang, Y.C., and Kim, T.H. (2001). A Modeling Method of a High Impedance Fault in a Distribution System Using Two Series Time-Varying Resistances in EMTP. In *2001 Power Engineering Society Summer Meeting. Conference Proceedings*, volume 2, 1175–1180. IEEE, Vancouver, BC, Canada.

Sedighi, A.R. and Haghifam, M.R. (2010). Simulation of High Impedance Ground Fault In Electrical Power Distribution Systems. In *2010 Int. Conf. Power Syst. Technol*, 1–7. doi:10.1109/POWERCON.2010.5666061.

Sheng, Y. and Rovnyak, S.M. (2004). Decision tree-based methodology for high impedance fault detection. *IEEE Transactions on Power Delivery*, 19(2), 533–536.

Soheili, A., Sadeh, J., and Bakhshi, R. (2018). Modified FFT based high impedance fault detection technique considering distribution non-linear loads: Simulation and experimental data analysis. *Int. J. Electr. Power Energy Syst.*, 94, 124–140. doi:10.1016/j.ijepes.2017.06.035.

Torres-Garcia, V., Guillen, D., Olveres, J., Escalante-Ramirez, B., and Rodriguez-Rodriguez, J.R. (2020). Modelling of high impedance faults in distribution systems and validation based on multiresolution techniques. *Computers Electrical Engineering*, 83, 106576. doi:https://doi.org/10.1016/j.compeleceng.2020.106576.

Trondoli, L., Lopes, G., and Vieira, J. (2022). Configurable stochastic model for high impedance faults simulations in electrical distribution systems. *Electric Power Systems Research*, 205, 107686. doi:https://doi.org/10.1016/j.epsr.2021.107686.

Wai, D.C.T. and Yibin, X. (1998). Novel Technique for High Impedance Fault Identification. *IEEE Transactions on Power Delivery*, 13(3), 676–686.